BOREAL ENVIRONMENT RESEARCH 21: 345–362
ISSN 1239-6095 (print) ISSN 1797-2469 (online)

Helsinki 23 May 2016

# Characteristics of new-particle formation at three SMEAR stations

Marko Vana[1)], Kaupo Komsaare[1)], Urmas Hõrrak[1)], Sander Mirme[1)], Tuomo Nieminen[2)3)], Jenni Kontkanen[2)], Hanna E. Manninen[2)], Tuukka Petäjä[2)], Steffen M. Noe[4)] and Markku Kulmala[2)]

[1)] *Institute of Physics, University of Tartu, Ülikooli 18, EE-50090 Tartu, Estonia*
[2)] *Department of Physics, P.O. Box 64, FI-00014 University of Helsinki, Finland*
[3)] *Department of Applied Physics, University of Eastern Finland, P.O. Box 1627, FI-70211 Kuopio, Finland*
[4)] *Institute of Agricultural and Environmental Sciences, Estonian University of Life Sciences, EE-51014 Tartu, Estonia*

*Received 30 Nov. 2015, final version received 18 Apr. 2016, accepted 19 Apr. 2016*

Vana M., Komsaare K., Hõrrak U., Mirme S., Nieminen T., Kontkanen J., Manninen H.E., Petäjä T., Noe S.M. & Kulmala M. 2016: Characteristics of new-particle formation at three SMEAR stations. *Boreal Env. Res.* 21: 345–362.

We analyzed the size distributions of atmospheric aerosol particles measured during 2013–2014 at Värriö (SMEAR I) in northern Finland, Hyytiälä (SMEAR II) in southern Finland and Järvselja (SMEAR-Estonia) in Estonia. The stations are located on a transect spanning from north to south over 1000 km and they represent different environments ranging from subarctic to the hemi-boreal. We calculated the characteristics of new-particle-formation events, such as the frequency of events, growth rate of nucleation mode particles, condensation and coagulation sinks, formation rate of 2 nm and 3 nm particles, and source rate of condensable vapors. We observed 59, 185 and 108 new-particle-formation events at Värriö, Hyytiälä and Järvselja, respectively. The frequency of the observed events showed an annual variation with a maximum in spring. The analysis revealed size dependence of growth rate at all locations. We found that the growth rate and source rate of a condensable vapor were the highest in Järvselja and the lowest in Värriö. The condensation sink and particle formation rate were of a similar magnitude at Hyytiälä and Järvselja, but several times smaller at Värriö. Tracking the origin of air masses revealed that the number concentration of nucleation mode particles (3–25 nm) varied from north to south, with the highest concentrations at Järvselja and lowest at Värriö. Trajectory analysis indicated that new-particle-formation events are large-scale phenomena that can take place concurrently at distant stations located even 1000 km apart. We found a total of 26 days with new-particle-formation events occurring simultaneously at all three stations.

## Introduction

New-particle-formation (NPF) in the atmosphere is an important phenomenon affecting many environmental aspects. By generating new particles, which can grow up to the sizes of cloud condensation nuclei (CCN), it influences cloud formation, and Earth's radiative balance, which

*Editor in charge of this article: Veli-Matti Kerminen*

in turn affect weather and climate (e.g. Kazil *et al*. 2010). Furthermore, NPF has an effect on atmospheric pollution, air quality and human health (Pope and Dockery 2006, Anderson 2009). Measurements of sub-3 nm particles are crucial to understanding the initial steps of atmospheric aerosol formation via gas-to-particle conversion, including aerosol nucleation (Kulmala *et al*. 2007, 2014). Besides knowing the concentrations of sub-3 nm neutral and charged particles that are formed during intensive and quiet periods of nucleation, assessment of their chemical composition and the concentrations of gaseous compounds participating in their formation and growth are essential to understand the process (Zhang *et al*. 2012, Kulmala *et al*. 2013, Tammet *et al*. 2013, 2014). Assessing the physical parameters of NPF is important. These characteristics can be used in different process models of aerosol particle genesis, as well as to improve climate and weather prediction models (e.g. Tunved *et al*. 2006a, Leppä *et al*. 2011, 2013, Luts *et al*. 2015, Lee *et al*. 2013, Mikkonen *et al*. 2011). Characteristics of NPF events depend on the location and environmental conditions. Therefore, for general understanding of NPF, measurements of the aerosol particle size distribution and air ion mobility distribution are needed at different locations.

To date, NPF characteristics have been studied at the SMEAR (Station for Measuring Ecosystem–Atmosphere Relations) stations in Hyytiälä and Värriö (Mäkelä *et al*. 1997, Kulmala *et al*. 1998, 2001, Vana *et al*. 2004, Dal Maso *et al*. 2005, Hirsikko *et al*. 2007, Hõrrak *et al*. 2008, Kyrö *et al*. 2014), as well as at some other locations around the globe (e. g. Hõrrak *et al*. 1998, Dal Maso *et al*. 2007 and 2008, Vana *et al*. 2008, Manninen *et al*. 2010, Vakkari *et al*. 2011, Hirsikko *et al*. 2011, 2012). Also several inter-comparison studies covering different sites in the boreal-forest zone and northern Scandinavia (e.g. Tunved *et al*. 2006b, Väänänen *et al*. 2013, Kristensson *et al*. 2014) were conducted. The SMEAR-Estonia station (located in Järvselja, Estonia) is a new addition to the SMEAR network, hence NPF events have not yet been thoroughly analyzed at that location.

We studied the NPF events taking place at Järvselja and compared the results with those from two measurement sites in Finland. A similar study was already performed for another Estonian measurement site in Tahkuse (*see* Vana *et al*. 2004). In the present study, however, a longer time series, advanced instrumentation and updated methods for calculating the quantitative characteristics of NPF events were applied.

The present study was based on the measurements of air ion and aerosol particle size distributions at Värriö (SMEAR I), Hyytiälä (SMEAR II) and Järvselja (SMEAR-Estonia). All the measurement sites are located in sparsely-populated, rural regions. The aim of this study was to find differences and similarities in NPF by comparing quantitative characteristics of the formation and growth events of nucleation mode aerosol particles at different locations. The measurement period used in our analysis was 1 Jan. 2013–31 Dec. 2014 when the aerosol particle measurement data were available from all the three stations. In this study, we considered the following characteristics of NPF events: (1) frequency of events, (2) growth rate (GR) of nanoparticles and its dependence on the particle size, (3) condensation sink (CS), (4) coagulation sink, (5) formation rates of 2-nm and 3-nm particles ($J_2$ and $J_3$, respectively), and (6) source rate of condensable vapor ($Q$). We also studied the seasonal and inter-annual variations in the concentrations of aerosol particles and air ions, including their number size distributions as well as the discrepancies and similarities in the data from different sites. Finally, we investigated the spatial extent of NPF through the detection of simultaneous NPF events at the three stations. We used back-calculated air-mass trajectories to describe the variation of NPF along the north to south transect, and the clearest NPF events with continuous growth of particles to characterize the regional extent of NPF. Our data set provided a unique opportunity to better characterize this horizontal extent based on a two years of data.

## Material and methods

### Measurement sites

The SMEAR I measurement station is located in Värriö (67°46´N, 29°36´E) in eastern Lapland,

Finland (for detials *see* e.g. Vehkamäki *et al*. 2004, Kyrö *et al*. 2014). The station is located on the top of a hill, Kotovaara, 390 m a.s.l. and is surrounded by a 60-year-old Scots pine forest. There are no towns or industry close by and thus practically no local air pollution. However, emissions from the mining industry in the Kola Peninsula in Russia can result in the elevated concentrations of pollutants when winds are transporting air from this region (Ruuskanen *et al*. 2007, Kaasik *et al*. 2011, Kyrö *et al*. 2014).

The SMEAR II measurement station (181 m a.s.l.) is located in Hyytiälä (61°51´N, 24°17´E) in the boreal-forest zone in southern Finland (for detials *see* Hari and Kulmala 2005). The station is surrounded by a rather homogeneous coniferous boreal forest and located fairly far from urban pollution sources. The new-particle formation and growth are frequently observed at Hyytiälä, especially in spring and autumn (Dal Maso *et al*. 2005). The measurements have been carried out since 1996 (e.g. Mäkelä *et al*. 1997, Nieminen *et al*. 2014).

The SMEAR-Estonia measurement station (36 m a.s.l.) is located near Järvselja (a village with fewer than 50 inhabitants) in Estonia (for detials *see* Noe *et al*. 2011, 2012, 2016). Järvselja (58°16´N, 27°16´E) is situated in the hemi-boreal forest zone with a moderately cool and moist climate, and is surrounded by a mixed forest.

SMEAR-Estonia is presently the southernmost station in the SMEAR network, extending over about 1000 km from the subarctic station in Värriö (SMEAR I), through Kuopio (SMEAR IV), Hyytiälä (SMEAR II) and urban station in Helsinki (SMEAR III) to the temperate zone, in Estonia(*see* https://www.atm.helsinki.fi/SMEAR/). This network of stations enables investigation of aerosol formation and transformation when the air masses pass along this long-distance route (Nilsson *et al*. 2001, Vana *et al*. 2004).

## Instrumentation

In Hyytiälä and Värriö, we measured the number size distributions of atmospheric aerosol particles by using a Differential Mobility Particle Sizer (DMPS). DMPS measures the size distribution of the total aerosol particle concentration including both neutral and charged particles. The DMPS system is a well-known stepwise scanning instrument, containing two Hauke-type differential mobility analyzers (DMA) of different length (10.9 and 28 cm), closed-loop sheath-flow arrangement and two different CPCs (TSI models 3010 and 3025) (Aalto *et al*. 2001, Dal Maso *et al*. 2005). Two DMPSs have partly overlapping size ranges to enable detection of particles of 3–1000 nm in diameter. This size range is divided into 38 logarithmically-distributed size sections and one size distribution is measured in 10 min. The DMPS system was calibrated as described in Aalto *et al*. (2001).

In Järvselja, we measured the number size distribution of atmospheric aerosol particles from 3 nm to 10 $\mu$m with an Electrical Aerosol Spectrometer (EAS), a multichannel instrument, designed at the University of Tartu, Estonia (Tammet *et al*. 2002). It consists of two multichannel DMAs with 32 measuring channels in total, each of which is provided with an electrometer for the detection of the particles precipitated on the isolated sections of the two DMAs. Unipolar corona chargers are used for particle charging. Two DMAs with different charging units are needed to provide sufficient size resolution in the entire size range of 3 nm–10 $\mu$m. One DMA uses a weak field ion diffusion mechanism (diffusion charging) and the other a strong field ion impact mechanism (field charging) to detect the particles in the size ranges from 3 nm to 1 $\mu$m and 0.3 $\mu$m to 10 $\mu$m, respectively. The association of different charging mechanisms makes a wide size range possible. EAS uses a parallel-measurement principle by measuring all the fractions of a size distribution simultaneously. The signal is integrated and a spectrum is produced over five-minute intervals. EAS was calibrated using a special procedure based on the mathematical model of the spectrometer and the experimental determination of some free parameters of that model, using quasi-monodispersed standard aerosols with known size distribution (Tamm *et al*. 2003).

In Hyytiälä and Järvselja, we also measured the number size distribution of charged and neutral particles using a Neutral cluster and Air Ion Spectrometer (NAIS; for description of the instru-

ment *see* Manninen *et al*. 2009, and Mirme and Mirme 2013). NAIS is a successor of the multichannel Air Ion Spectrometer (AIS) developed at the University of Tartu in cooperation with Airel Ltd. (for description of the instrument *see* Mirme *et al*. 2007). NAIS consists of two multichannel DMAs, one for the measuring of air ions of positive and the other for negative polarity. Air ions are classified according to their electrical mobility and the electric currents they produce are measured by 21 integrating electrometers. Thus, the whole mobility distribution is simultaneously measured for both polarities. The mobility range of NAIS is 3.16–0.001 $cm^2\ V^{-1}\ s^{-1}$, which corresponds to a mobility diameter range of 0.8–42 nm (Millikan-Fuchs equivalent diameter; Mäkelä *et al*. 1996). Besides naturally-charged air ions, NAIS can also measure the size distribution of neutral particles in the diameter range ~2–42 nm. For particle measurements, NAIS uses software-controlled unipolar corona chargers for charging the particles. NAIS typically measures the air ion and total particle number distributions alternatively in a five-minute measurement cycles with two-minute integrating periods for either mode and one-minute for off-set signal measurements. For diameters above 3 nm, similarly as EAS, NAIS was calibrated using standard aerosols. NAIS has proved its performance for mobility and concentration measurements during a calibration and intercomparison workshop (Asmi *et al*. 2009, Gagné *et al*. 2011).

## Data analysis

### Classifying new-particle-formation events

Our results showed that new-particle-formation events were frequent at all the three sites. To characterize those NPF events, we need to classify them. So far, no unique mathematical criterion for the classification of the NPF events exists, although several attempts have been made (Kulmala *et al*. 2012). Therefore, we analyzed the data visually on a day-to-day basis for each 24-hour period, from midnight to midnight, and classified the events according to the evolution of the size distribution of aerosol particles. In several earlier studies in which the NPF events were observed, the above-mentioned visual classification method was applied successfully (e.g. Dal Maso *et al*. 2005, Hirsikko *et al*. 2007, Vana *et al*. 2008, Manninen *et al*. 2010).

We classified and grouped the NPF events observed between 1 Jan. 2013 and 31 Dec. 2014 into two classes (I and II) according to Dal Maso *et al*. (2005). Class I events can be further divided into subclasses Ia and Ib, in which class Ia events represent the most clear particle formation and growth event days, while class Ib events reveal a less clear particle growth in time. For class II events, we can identify a NPF event but the calculation of the growth and formation rates is not possible or it includes substantial uncertainties. We also had days when no NPF was identified. Those days were classified as non-event days. All other days were denoted as undefined. Rain events can also lead to enhanced concentrations of charged nanoparticles (intermediate air ions, preferably negatively charged) generated via the balloelectric effect (Tammet *et al*. 2009). Such events were not considered aerosol nucleation events in this study.

### Estimating air ion and particle growth rates

In order to find out characteristics of the NPF at the three sites and to study the regional nature of NPF events, we calculated the growth and formation rates of nucleation mode aerosol particles for class I events. This was because only those events that take place in the air masses of considerable horizontal extent enable the characterization of particle formation and growth rates.

We calculated the growth rate of nanoparticles using the maximum-concentration method (Hirsikko *et al*. 2005, Kulmala *et al*. 2012). According to this method, times when the concentration maximum reaches certain size bins are determined. In order to determine the concentration peaks, a normal (Gaussian) distribution function was fitted to the time series of the particle concentration in a certain size fraction (spectrometer channel). The ratio of differences between representative diameters and concentration peak times yields the value of growth rate, which represents the growing aerosol population.

## Particle formation rates

We calculated the formation rate of neutral particles $J_{dp}$ using the following formula (Kulmala *et al*. 2007, 2012, Manninen *et al*. 2010):

$$J_{dp} = \frac{dN_{dp}}{dt} + \mathrm{CoagS}_{dp} N_{dp} + \frac{\mathrm{GR}}{\Delta d_p} N_{dp}, \quad (1)$$

where $\mathrm{CoagS}_{dp}$ is the coagulation sink of particles in the diameter range $[d_p, d_p + \Delta d_p]$ with concentration of $N_{dp}$ and GR is their growth rate.

The formation rate of positively or negatively (indicated with superscript + or −, respectively) charged particles $J_{dp}^{\pm}$ is given by

$$J_{dp}^{\pm} = \frac{dN_{dp}^{\mp}}{dt} + \mathrm{Coag}S_{dp} N_{dp}^{\pm} + \frac{\mathrm{GR}}{\Delta d_p} N_{dp}^{\pm} + \alpha N_{dp}^{\pm} N_{<dp}^{\mp} - \chi N_{dp} N_{<dp}^{\pm}, \quad (2)$$

where, compared with Eq. 1, two additional terms are added. The fourth term on the right-hand side of the equation represents the ion–ion recombination and the fifth term represents the charging of neutral particles by smaller ions. $N_{<dp}^{\mp}$ and $N_{<dp}^{\pm}$ are the number concentrations of charged particles smaller in diameter than $d_p$ and $N_{dp}$ is the concentration of neutral particles in the diameter range $[d_p, d_p + \Delta d_p]$. In the present study, we assumed the ion–ion recombination coefficient, $\alpha$, and the ion-aerosol attachment coefficient, $\chi$, to be equal to $1.6 \times 10^{-6}$ cm$^3$ s$^{-1}$ and $0.01 \times 10^{-6}$ cm$^3$ s$^{-1}$, respectively (Tammet and Kulmala 2005).

We obtained the formation rate of 2-nm particles (Eq. 1) and air ions (Eq. 2) by using the NAIS number size distributions measured in the particle mode and ion mode, respectively. The NAIS instrument was available only in Hyytiäla and Järvselja. However, we were able to calculate the formation rate of 3-nm particles using aerosol size distribution data measured by DMPS or EAS.

## Condensation sink

The condensation sink (CS) describes the condensing vapor sink caused by an aerosol population. We used the aerosol particle size distribution data measured by DMPS to calculate the condensation sink values for Hyytiälä and Värriö, whereas the EAS number size distribution data were used to obtain the condensation sink values for Järvselja. We calculated the condensation sink from the measured number size distribution using the following formula (Kulmala *et al*. 2001, Dal Maso *et al*. 2002):

$$\mathrm{CS} = 2\pi D \int_0^{d_{p,\max}} d_p \beta_m \left(d_p\right) n\left(d_p\right) dd_p, \quad (3)$$
$$= 2\pi D \sum_i \beta_{m,i} d_{p,i} N_i$$

where $N_i$ is the particle number concentration for size class $i$, $D$ is the diffusion coefficient of a condensing vapor which is usually assumed to be sulfuric acid and $\beta_m$ represents a transition-regime correction factor that can be calculated using the scheme proposed by Fuchs and Sutugin (1971).

The condensation sink and growth rate of particles are interrelated with the source rate of condensable vapor. We can calculate the apparent source rate $Q$ with the following equation:

$$Q = \mathrm{CS} \times A \times \mathrm{GR}_{nuc}, \quad (4)$$

where $\mathrm{GR}_{nuc}$ is the growth rate of nucleation mode aerosol particles and $A$ is a constant having a value of $1.37 \times 10^7$ h cm$^{-3}$ nm$^{-1}$ for a vapor with the molecular properties of sulfuric acid (Dal Maso *et al*. 2005). We assumed that a growth rate of 1 nm h$^{-1}$ corresponds to a vapor concentration of $1.37 \times 10^7$ cm$^{-3}$.

## Analysis of an air mass origin

To study effects of air mass history on the new-particle formation we calculated 96-hour-long back-trajectories for all days of the measurement period. We used the HYSPLIT (Hybrid Single-Particle Lagrangian Integrated Trajectories; https://ready.arl.noaa.gov/HYSPLIT.php) model to estimate the origin of air masses passing the stations (Stein *et al*. 2015, Rolph 2016). The archived meteorological data from the NOAA Global Data Assimilation System (GDAS) were used. Three arrival heights of 100, 500 and 1000 m above ground level were chosen to cover the boundary layer during day and night time

and to find out if trajectories for different heights give additional information. Further input were the total run-time (96 h), the station coordinates (Hyytiälä: 61.85N, 24.283E; Värriö: 67.767N, 29.583E; Järvselja: 58.272N, 27.27E), and we chose vertical velocity method for the vertical motion calculation.

In order to connect the number concentration of the nucleation mode particles (3–25 nm) and the origin of air mass, we used a trajectory statistical method that combines *in situ* measurements of aerosol particle concentrations and back trajectories calculated for corresponding times. This method takes into account the uncertainty of trajectory and therefore the dispersion of particle concentration along the trajectory. Uncertainty is estimated to be 10%–30% of the distance traveled by the air parcel [15%–30% according to Heinzerling (2004) and 10%–20% according to Draxler and Hess (1998)]. At each time step (one hour), we first calculated the coordinates of two squares that surrounds a given trajectory point, the larger square with a side length of 20% and smaller square with 10% of the traveled distance. All cells (1° × 1°) inside those squares got weighted concentration values of 0.3 and 0.7 for the larger and smaller squares, respectively. To improve statistical significance, we took into account only cells that were passed by a minimum of 20 trajectories. When an air mass moves slower, the uncertainty or actually the dispersion of a trajectory is smaller. The method described above was used in the study made for Hyytiälä based on the trace gas and aerosol data collected in 1996–2008 (Riuttanen *et al*. 2013). In the present study, we used the hourly averages of the total number concentration of nucleation mode particles (3–25 nm in diameter) collected at the three locations. The hourly average was calculated using the data from 0.5 hours before and after full hour as it is also the arrival time of the trajectory.

## Results and discussion

### Statistics of particle formation events at three sites

We analyzed the data from a two-year period (2013–2014). However, the measurement instruments did not operate all the time, which caused some gaps in our data set (different for different stations and instruments). We calculated percentages of the time when the measurement data were available during 2013–2014 (Fig. 1). We had measurement data available for at least 70% of the two-year period depending on the instrument (DMPS, NAIS, EAS). For the DMPS measurements, the data availability was more than 94%. There were periods when instruments did not measure or the measurement data did not pass the quality control (some diagnostic parameters of the instruments were out of range or measured concentrations did not have realistic values). We can also see the periods when the NPF events (class I and II) occurred at different locations (Fig. 1).

The new-particle-formation events (classes I and II) were detected on 59, 185 and 108 days in Värriö, Hyytiälä and Järvselja, respectively (Table 1). Of those days, about 21%, 43% and 34% consisted of class I events at Värriö, Hyytiälä and Järvselja, respectively. The fraction of the classified days (all event days and non-event days) having a NPF event (class I or II) was about 43% at Hyytiälä, which is similar to the fraction (45%) reported by Dal Maso *et al*. (2005). The corresponding fractions in Värriö and Järvselja were smaller: 13% and 37%, respectively. Kyrö *et al*. (2014) reported that during 1998–2011 the number of NPF events at Värriö was on average 54 per year (of which 20 were class I events for which it was possible to determine both growth and formation rates). There were about 59 NPF events (out of which 12 were class I events) during 2013–2014 in Värriö (Table 1). The number of non-event days (404) was the highest at Värriö where most of the days were non-event days. At Hyytiälä and Järvselja, the fraction of non-event days was relatively similar, being about 35% of all the measurement days.

We compared the observations of NPF frequency at Järvselja with the observations from the Aspvreten station (58°46´N, 17°24´E) located near the Swedish coastline in Sörmland, about 70 km south of Stockholm and 2 km from the seaside. Aspvreten is quite close to Järvselja and approximately at the same lat-

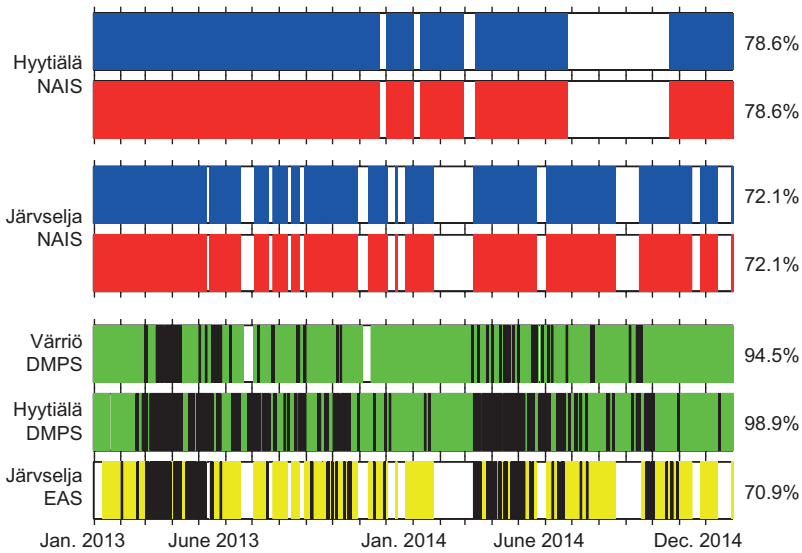


**Fig. 1**. The periods with the measurement data available for Värriö, Hyytiälä and Järvselja during 2013–2014. The white gaps represent the periods when the instruments did not measure or the measurement data did not pass the quality control. For the NAIS data, the blue and red colors represent the negative and positive polarities, respectively. The black lines indicate the days when the NPF events (classes I and II) occurred. The percentages on the right-hand side of the figure indicated the part of the time when the instruments measured correctly.

itude. Dal Maso *et al*. (2007) reported that the fraction of the event days (the number of event days from all measurement days) at Aspvreten was 15.2%. The same fraction for Järvselja was 20.5% (Table 1).

We observed a clear seasonal cycle in NPF at all the three stations, and calculated an annual variation in the frequency of the NPF events (classes I and II) for these sites (Fig. 2). This frequency was calculated as the ratio between the number of events and all the days in a month. We also calculated the percentages of the time when the measurement data were available in each month (Fig. 2). The frequency of the event days had a clear seasonal pattern: the number of the NPF event days had a maximum in March and minimum in December–January. The frequency was the highest at Hyytiälä and the lowest at Värriö, whereas the frequency at Järvselja was intermediate. However, the frequencies at Järvselja and Hyytiälä, beside the main peaks in the early spring (March), also had second maxima in autumn (September–October). This feature was not as clear in the Värriö data because a comparatively high number of NPF events at this site took place also during the summer. Similar annual patterns of two maxima were recorded at the Tahkuse station in Estonia (Hõrrak *et al*. 2000), and at Hyytiälä and Värriö (e.g. Dal Maso *et al*. 2005, Vehkamäki *et al*.

**Table 1**. Statistics of NPF events based on the measurements at Värriö, Hyytiälä and Järvselja during 2013–2014.

| | Numbers of days | | | Percentage of all days | | | Percentage of measurement days | | |
|---|---|---|---|---|---|---|---|---|---|
| | Värriö | Hyytiälä | Järvselja | Värriö | Hyytiälä | Järvselja | Värriö | Hyytiälä | Järvselja |
| Class I | 12 | 79 | 37 | 1.6 | 10.8 | 5.1 | 1.7 | 11.0 | 7.0 |
| Class II | 47 | 106 | 71 | 6.4 | 14.5 | 9.7 | 6.8 | 14.7 | 13.5 |
| Non-events | 404 | 247 | 182 | 55.4 | 33.9 | 24.9 | 58.7 | 34.2 | 34.6 |
| Undefined | 226 | 289 | 236 | 31.0 | 39.6 | 32.3 | 32.8 | 40.1 | 44.9 |
| Measurement days | 689 | 721 | 526 | 94.4 | 98.8 | 72.0 | 100 | 100 | 100 |

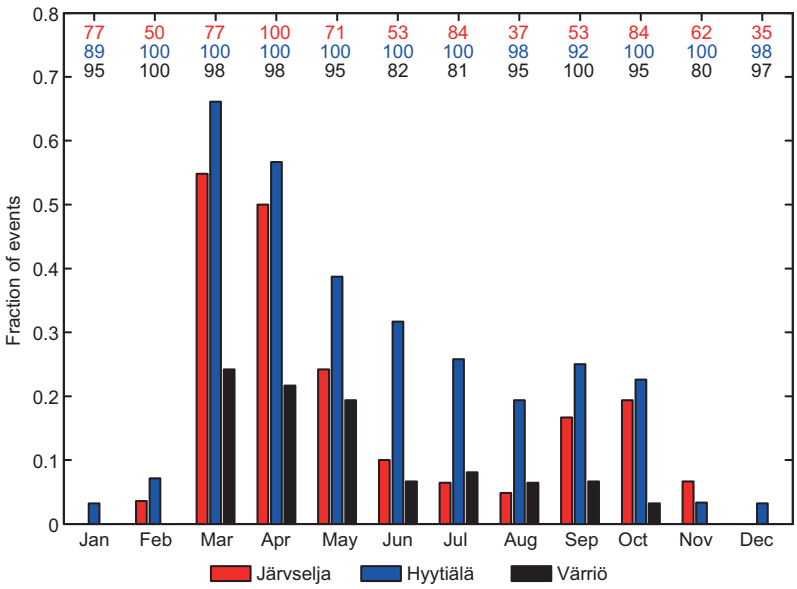


**Fig. 2**. Comparison of the annual variation in the frequency of the NPF event days (classes I and II) at Järvselja, Hyytiälä and Värriö during 2013–2014. The frequency is the ratio between number of events and all days in month. The numbers at the top of the figure are the percentages of the time when the measurement data were available.

2004, Kyrö *et al*. 2014). In the north-European countries, the annual variation in aerosol nucleation events can be explained by changes in the inflow of the Arctic air masses creating favorable conditions for the photochemical aerosol nucleation: the low condensation and coagulation sinks and relatively high sun radiation intensity (e.g. Nilsson *et al*. 2001, Tunved *et al*. 2003, Wehner *et al*. 2007, Hussein *et al*. 2009).

## Observed growth and formation rates

We calculated GR for three size classes (1.6–3 nm, 3–7 nm and 7–25 nm) using the NAIS data (air ion measurement mode) from Hyytiälä and Järvselja. The DMPS data were used to calculate GR in the nucleation mode size range 3–25 nm for Hyytiälä and Värriö. The EAS data were used to calculate GR in the nucleation mode size range for Järvselja. We found that GR increased with an increasing particle size at Hyytiälä and Järvselja. The average values of GR, when considering both positive and negative ion analyzer measurements obtained from NAIS (Table 2), were 2.3, 3.8 and 4.6 nm $h^{-1}$ at Hyytiälä and 3.4, 5.2 and 7.1 nm $h^{-1}$ at Järvselja in the size ranges of 1.6–3 nm, 3–7 nm and 7–25 nm, respectively. The corresponding median values of GR were 1.5, 3.1 and 3.8 nm $h^{-1}$ at Hyytiälä and 2.6, 4.0 and 6.1 nm $h^{-1}$ at Järvselja. Typical values of GR at Järvselja were thus about 1.5 times greater than those at Hyytiälä. The EAS and DMPS measurements indicated even a higher ratio of about 2.

A size-dependent growth rate for nucleation mode particles have been reported by earlier studies (e.g. Hirsikko *et al*. 2005, Iida *et al*. 2008, Manninen *et al*. 2010, Kuang *et al*. 2012, Kulmala *et al*. 2013). The size dependency of GR suggests that there could be different condensing vapors participating in the growth of particles of different sizes depending on the compound saturation vapor pressures, resulting in the increase in GR with and increasing size in the range of 1.6–25 nm. In our study, the values of GR in the size range of 3–25 nm were the highest at Järvselja (on average 3.5–7.5 nm $h^{-1}$) and the smallest at Värriö (on average 1.8 nm $h^{-1}$). Kyrö *et al*. (2014) reported average GR of particles during the nucleation event days being 2.7 nm $h^{-1}$ during 1998–2011 at Värriö. At Hyytiälä, average GRs were in the range of 2.2–4.7 nm $h^{-1}$ (Table 2). The median values of GRs were always somewhat smaller than the average values.

We evaluated the diurnal variation in the formation rates of 2-nm neutral and charged particle for Hyytiälä and Järvselja by applying the NAIS measurements (Fig. 3). The daily cycles

of $J_2$, $J_2^-$ and $J_2^+$ for the class I event days were very similar at Hyytiälä and Järvselja. In general, the values of $J_3$ were about 60% and 80% of those of $J_2$ at Hyytiälä and Järvselja, respectively (Table 2). On average, the values of $J_2^-$ and $J_2^+$ were both about 2 percentage points from the values of $J_2$ at Hyytiälä, while at Järvselja the corresponding value of $J_2^-$ was about 4 percentage points. On average, $J_3$ was several times higher at Hyytiälä (0.93 $cm^{-3}$ $s^{-1}$) and Järvselja (1.17 $cm^{-3}$ $s^{-1}$) as compared with that at Värriö (0.15 $cm^{-3}$ $s^{-1}$). Kyrö *et al*. (2014) found that the average formation rate of 3 nm particles during 2005–2011 at Värriö was 0.24 $cm^{-3}$ $s^{-1}$. In our study, the values of $J_2$, $J_2^-$ and $J_2^+$ were similar at Hyytiälä and Järvselja. On average, $J_2$ was slightly higher at Hyytiälä (1.49 $cm^{-3}$ $s^{-1}$) than at Järvselja (1.30 $cm^{-3}$ $s^{-1}$). Kulmala *et al*. (2012) reported $J_2$ and $J_3$ to be 1.1 $cm^{-3}$ $s^{-1}$ and 0.61 $cm^{-3}$ $s^{-1}$, respectively, for a typical class I NPF event detected at Hyytiälä. Our results on $J_3$ and diurnal cycles of $J_2$, $J_2^-$ and $J_2^+$ at Hyytiälä agree with the results of Kulmala *et al*. (2013).

The relationship between $J_2$ and $J_3$ can be estimated by taking into account the condensational growth and coagulation scavenging as follows (Kerminen and Kulmala 2002, Kulmala *et al*. 2012):

$$J_3 = J_2 \exp\left[\gamma\left(\frac{1}{3}-\frac{1}{2}\right)\frac{CS}{GR_{2-3}}\right], \quad (5)$$

where $GR_{2-3}$ is the growth rate of nucleated particles from 2 nm to 3 nm and $\gamma$ is to equal 0.23 $nm^2$ $m^2$ $h^{-1}$. We used Eq. 5 to calculate $J_3$ form $J_2$ for Hyytiälä and Järvselja (Table 2). The values of $J_3$ calculated using Eq. 5 were in good agreement with those calculated using Eq. 1 for both stations.

## Effect of condensation sink on NPF

Similarly to GRs of nucleation mode particles, the condensation sink during the NPF days increased from north to south, with the smallest values recorded at Värriö and the highest ones at Järvselja (Table 2).

We determined the annual variation in the condensation sink at Värriö, Hyytiälä and Järvselja using Eq. 3, and found that condensation sinks at Järvselja (mean = 3.2–5.5 × $10^{-3}$ $cm^{-3}$ $s^{-1}$) and Hyytiälä (mean = 3.0–6.5 ×

**Table 2**. The averages, medians and standard deviations of the growth rates (GR) (nm $h^{-1}$), formation rates ($J$, $cm^{-3}$ $s^{-1}$), condensation sinks (CS) ($10^{-3}$ $s^{-1}$) and source rates of condensable vapor ($Q$, $10^3$ $cm^{-3}$ $s^{-1}$) for the NPF days at Värriö, Hyytiälä and Järvselja during 2013–2014. The values of GR are given in the size range 3–25 nm for neutral particles and in three size ranges for both negative (–) and positive (+) ions. In the first column, the instruments used to gather data for the calculations are given in parentheses. $J_3$* is the formation rate calculated using Eq. 5. The number of counted measurements was 12, 61 and 36 for Värriö, Hyytiälä and Järvselja, respectively.

| | Värriö | | | Hyytiälä | | | Järvselja | | |
|---|---|---|---|---|---|---|---|---|---|
| | Mean | Median | SD | Mean | Median | SD | Mean | Median | SD |
| GR, 3–25 nm (DMPS/EAS) | 1.8 | 1.6 | 0.9 | 2.5 | 2.1 | 1.9 | 5.4 | 4.6 | 2.8 |
| GR, ions, < 3 nm (NAIS) | – | – | – | 2.2 | 1.2 | 2.6 | 3.1 | 2.2 | 2.5 |
| GR, – ions, 3–7 nm (NAIS) | – | – | – | 3.8 | 3.1 | 2.6 | 4.5 | 3.1 | 4.5 |
| GR, – ions, 7–25 nm (NAIS) | – | – | – | 4.5 | 3.7 | 2.1 | 6.6 | 5.4 | 6.6 |
| GR, + ions, < 3 nm (NAIS) | – | – | – | 2.4 | 1.8 | 2.5 | 3.6 | 2.9 | 2.7 |
| GR, + ions, 3–7 nm (NAIS) | – | – | – | 3.7 | 3.1 | 2.0 | 5.8 | 4.8 | 5.8 |
| GR, + ions, 7–25 nm (NAIS) | – | – | – | 4.7 | 3.9 | 2.6 | 7.5 | 6.7 | 7.5 |
| $J_3$ (DMPS/EAS) | 0.15 | 0.14 | 0.05 | 0.93 | 0.56 | 0.87 | 1.17 | 0.81 | 1.00 |
| $J_3$* | – | – | – | 0.96 | 0.70 | 0.73 | 1.12 | 0.87 | 1.00 |
| $J_2$ (NAIS) | – | – | – | 1.49 | 1.08 | 1.05 | 1.30 | 1.09 | 1.06 |
| $J_2^-$ (NAIS) | – | – | – | 0.03 | 0.03 | 0.02 | 0.06 | 0.05 | 0.04 |
| $J_2^+$ (NAIS) | – | – | – | 0.03 | 0.02 | 0.01 | 0.03 | 0.03 | 0.02 |
| CS | 0.8 | 0.6 | 0.6 | 2.8 | 2.0 | 2.3 | 2.9 | 2.7 | 1.1 |
| $Q$ | 22 | 17 | 18 | 116 | 59 | 159 | 217 | 179 | 131 |

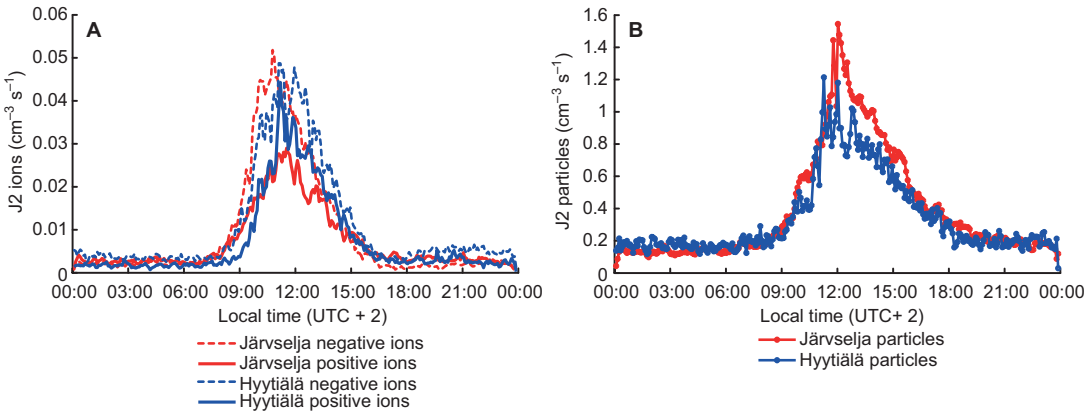


**Fig. 3**. The diurnal variation of the median formation rates for class I event days at Järvselja and Hyytiälä during 2013–2014. (**A**) The ion formation rates ($J_2^-$ and $J_2^+$), and (**B**) the total particle formation rates ($J_2$). All the formation rates of 2-nm particles were calculated using the NAIS data.

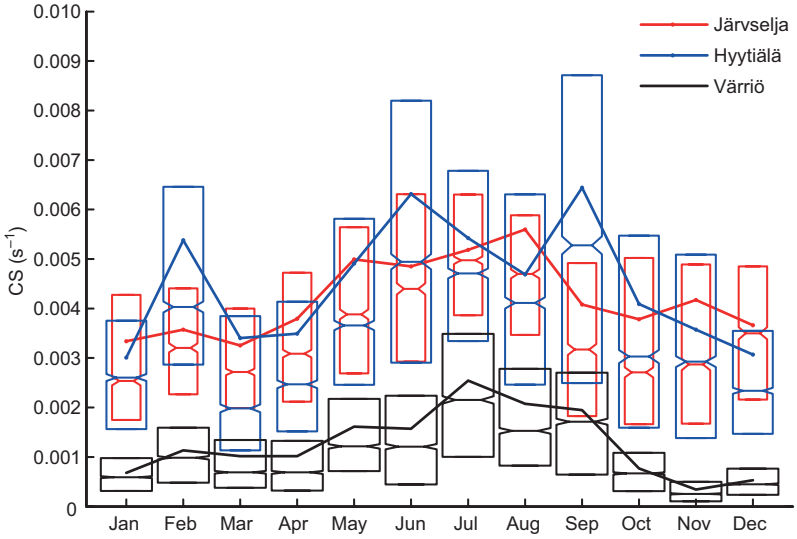


**Fig. 4**. The annual variation in the condensation sink (CS) for Järvselja, Hyytiälä and Värriö during 2013–2014. The solid lines represent the average values and the boxes (from bottom to top), lower quartile (25%), median (50%) and upper quartile (75%). The notches mark the 95% confidence intervals for the medians. The numbers of available data for the stations are given in Fig. 2.

$10^{-3}$ cm$^{-3}$ s$^{-1}$) were similar, but much smaller at Värriö (mean = 0.2–2.5 × $10^{-3}$ cm$^{-3}$ s$^{-1}$) (Fig. 4). The NPF frequency varied in an opposite phase to that of CS (Figs. 2 and 4). As a result, we can conclude that a high value of CS decreases the probability of NPF to occur. CS had the highest values during summer, which may suppress NPF. However, CS was also quite high in September at Hyytiälä and Värriö. Here, the main factor that limited NPF was presumably the ratio of the concentration of condensable vapors (e.g. sulfuric acid and extreme low volatile organics), or their source rate ($Q$), to CS.

We calculated the median diurnal variation of the condensation sink separately for class I NPF event days and non-event days for the three stations. The values of CS were usually about 1.5–3 times higher on non-event days as compared with those on the event days (Fig. 5). This difference was the highest between 09:00 21:00 when the formation and growth of new particles usually occur. During the event days, CS showed a clear diurnal pattern at Hyytiälä and Värriö, but during the non-event days, CS varied very little.

We determined the source rate of condensable vapor ($Q$) by using Eq. 4 (Table 2). The high-

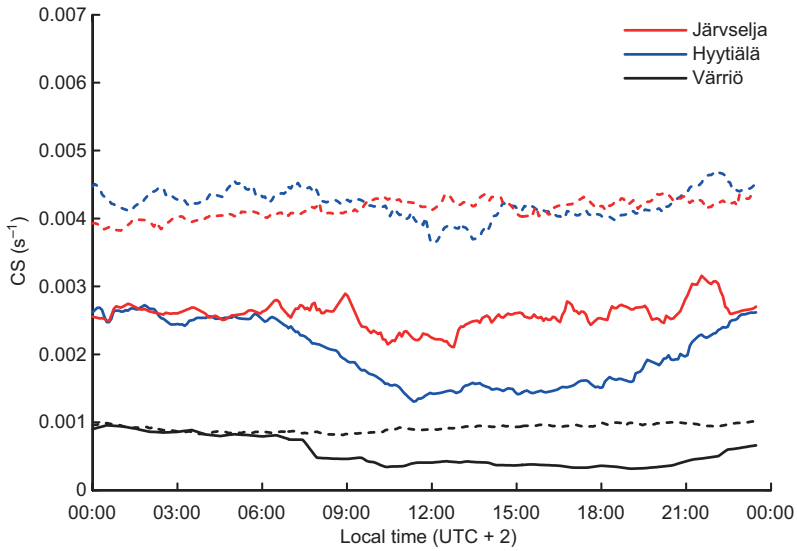


**Fig. 5**. The diurnal variations in the median condensation sink (CS) for class I event days (solid lines) and non-event days (dashed lines) at the three stations during 2013–2014.

est source rates were obtained for Järvselja (on average $2 \times 10^5$ cm$^{-3}$ s$^{-1}$), since the growth rate of nucleation mode particles was the highest there. The lowest source rates were obtained for Värriö (on average $2 \times 10^4$ cm$^{-3}$ s$^{-1}$). At Hyytiälä, the source rate was on average $1 \times 10^5$ cm$^{-3}$ s$^{-1}$, which is in good agreement with the previous study of Dal Maso *et al*. (2005) who found the vapor source rate to vary between $10^4$ and $10^6$ cm$^{-3}$ s$^{-1}$.

Of all the three stations, the lowest values of condensation sink, NPF frequency, formation and growth rates and source rate of condensable vapor were obtained for Värriö. This is indicative of a link between the sources and sinks for gaseous precursors. In Värriö, the low values of CS can be associated with the lack of precursors, which does not promote NPF.

## Effect of air mass history on NPF

We calculated the 96-hour-long air mass back-trajectories for the event days (Fig. 6A) and non-event days (Fig. 6B). On the event days, air masses traveled mostly from north to south or from northwestern directions over Scandinavia. On the non-event days, however, the air was most often moving from south to north. At least at Hyytiälä and Järvselja, the southerly directions were dominant and the trajectories closer to stations did form specific corridors.

We used a trajectory statistical method that combines *in situ* measurements of aerosol particle concentrations and back trajectories for all three measurement stations (*see* section "Analysis of air mass origin"). As a result, the number concentration fields of nucleation mode particles (3–25 nm) according to transport directions of air masses were obtained for the three measurement stations (Fig. 7). Figure 7 depicts the distribution of nucleation mode particle concentration measured at one particular station by the air mass transport back-trajectories statistically averaged over 2013–2014, not the geographical distribution of nucleation mode aerosol particles transported to the station, since the atmospheric lifetime of those particles is typically shorter than few hours. However, it can be interpreted as presenting a distribution of the sum of factors (gaseous precursors, preexisting aerosol particles, meteorological parameters, etc.) providing favorable conditions for NPF along the transport trajectories.

The variation in NPF along the north to south transect is evident (Fig. 7). The highest concentrations of nucleation mode particles occurred at Järvselja, the lowest ones at Värriö and intermediate at Hyytiälä. At all the stations, the highest concentrations were found when air masses moved over the measurement location from northerly directions. Our results illustrate the effect shown for the northern Europe by

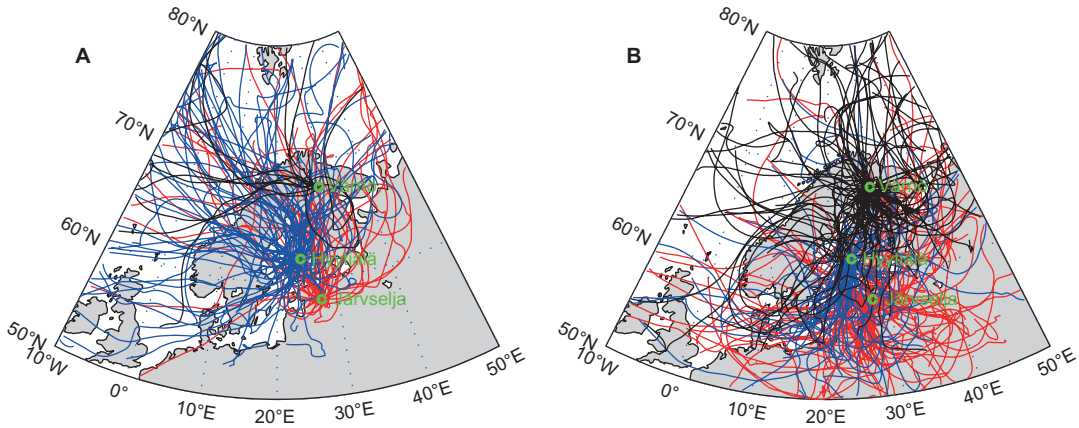


**Fig. 6**. The air mass 96-hour-long back-trajectories ending in Värriö (black), Hyytiälä (blue) and Järvselja (red) for (**A**) class I event days, and (**B**) non-event days during 2013–2014. The trajectories were calculated for the arrival height of 100 m a.s.l. and arrival time of 10:00 UTC.

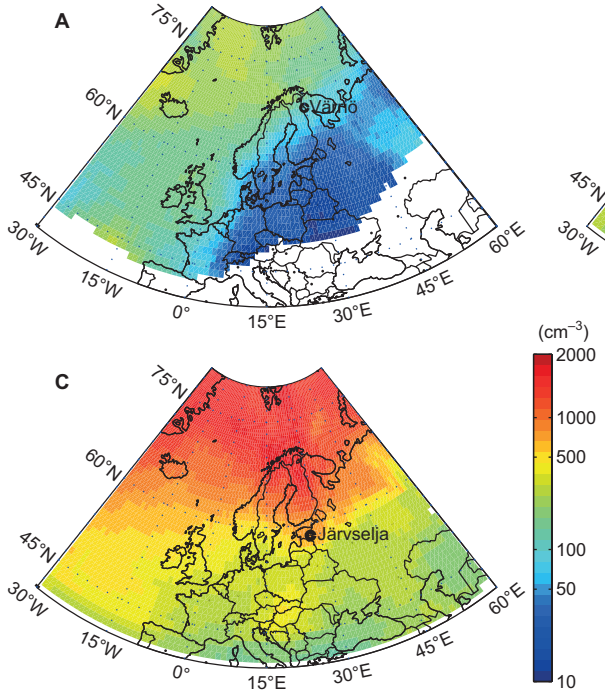


**Fig. 7**. The number concentration fields of nucleation mode particles (3–25 nm) according to transport directions of air masses for (**A**) Värriö, (**B**) Hyytiälä and (**C**) Järvselja during 2013–2014. The numbers of counted trajectories were 8748, 8748 and 8758 for Värriö, Hyytiälä and Järvselja, respectively.

Tunved *et al*. (2006b): when Arctic air masses move to the continental area from north to south, they typically spent more time over land (boreal forest) than other air masses, which is accompanied by generation of new particles and their growth to climatically-relevant sizes.

In order to find out whether NPF is a regional-scale phenomenon, we studied the NPF events occurring simultaneously at all the three stations. We searched for cases in which the concentration of nucleation mode particles was two times greater than the corresponding two-year-average concentrations for at least two hours during the same day at all the stations. The calculations for the two-year average included all measurement days. The two-year average concentrations for aerosol particles in the size range of 3–25 nm were 150 cm$^{-3}$, 450 cm$^{-3}$ and 800 cm$^{-3}$ at Värriö,

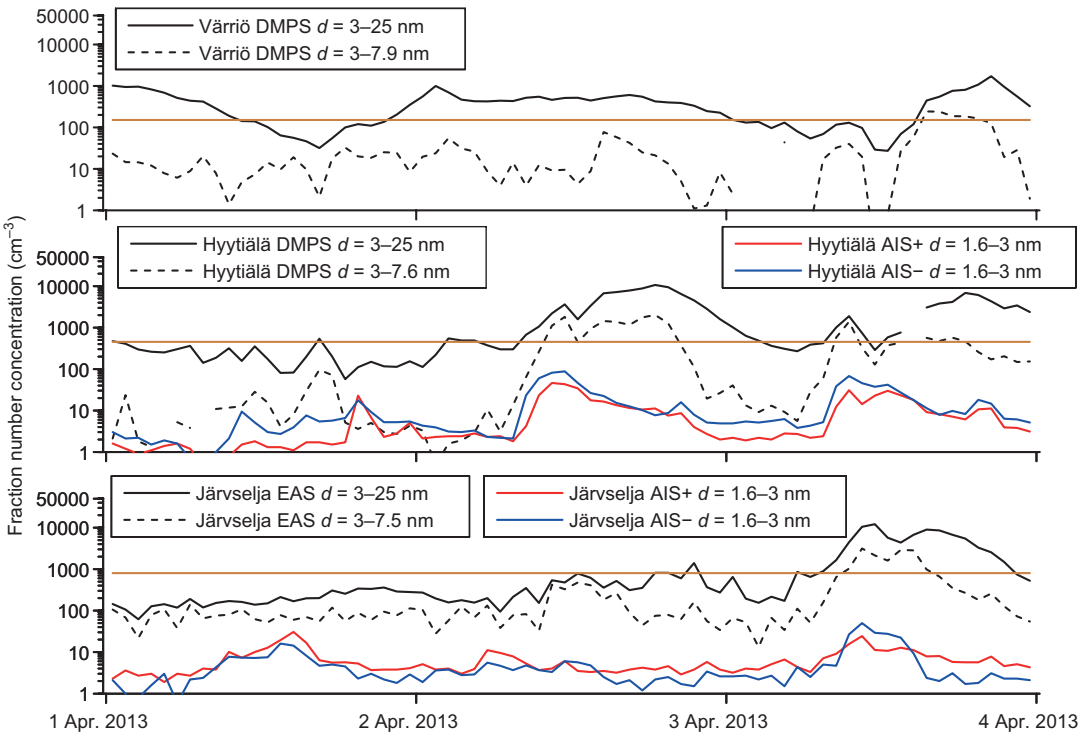


**Fig. 8**. The time variations of the size fractions number concentrations of recently-formed aerosol particles at the three measurement locations during 1–3 April 2013. In the case of the EAS and DMPS data, the total concentration of aerosol particles (charged and neutral) in a given size range is indicated, but in the case of NAIS only charged particles (ions) are given. The brown, horizontal line indicates the two-year average number concentration of nanometer particles in the size range of 3–25 nm.

Hyytiälä and Järvselja, respectively. According to this criterion, the total number of the days when a NPF event occurred at all the stations and exceeded the above-mentioned concentration thresholds was 26 (19 in 2013 and 7 in 2014). We recorded all those episodes during spring (between March and May).

Finally, we investigated one of the typical situations of a NPF event occurring at all the three stations during the same day to study whether such NPF event is a synoptic-scale phenomenon (Figs. 8 and 9). When the air mass originated from nearly the same direction (sector) from the Arctic, the NPF event occurred at all the stations (3 April 2013). The air mass that introduced a NPF event at one station moved to another station during one day and also developed a NPF event at that station: the successive development of NPF during three days from 1 April to 3 April 2013 when the Arctic air mass passed from north to south (from Värriö to Järvselja; Fig. 9) is depicted in Fig. 8. NPF seems to take place in northern air masses originating from Arctic, since the process occurred at Hyytiälä and Järvselja when the air mass origin changed from south to north (*see* also Fig. 6). The total concentration of newly-formed particles during a NPF event tends to increase when the Arctic, maritime air mass moves towards the south over land. The air mass moving from the Arctic Sea towards the continent creates favorable conditions for NPF. Therefore, the event can be recorded at the continental station after passage of a cold front, or with some delay depending on the intensity of photochemical processes, which are the main reason for the daytime enhancement of the nucleation mode particle concentration. So, depending on the movement of an air mass (the invasion depth form Arctic to mid latitude), a NPF event was first recorded at Värriö, then at Hyytiälä, and eventually at Järvselja, as they all became engulfed in the same air mass. Some

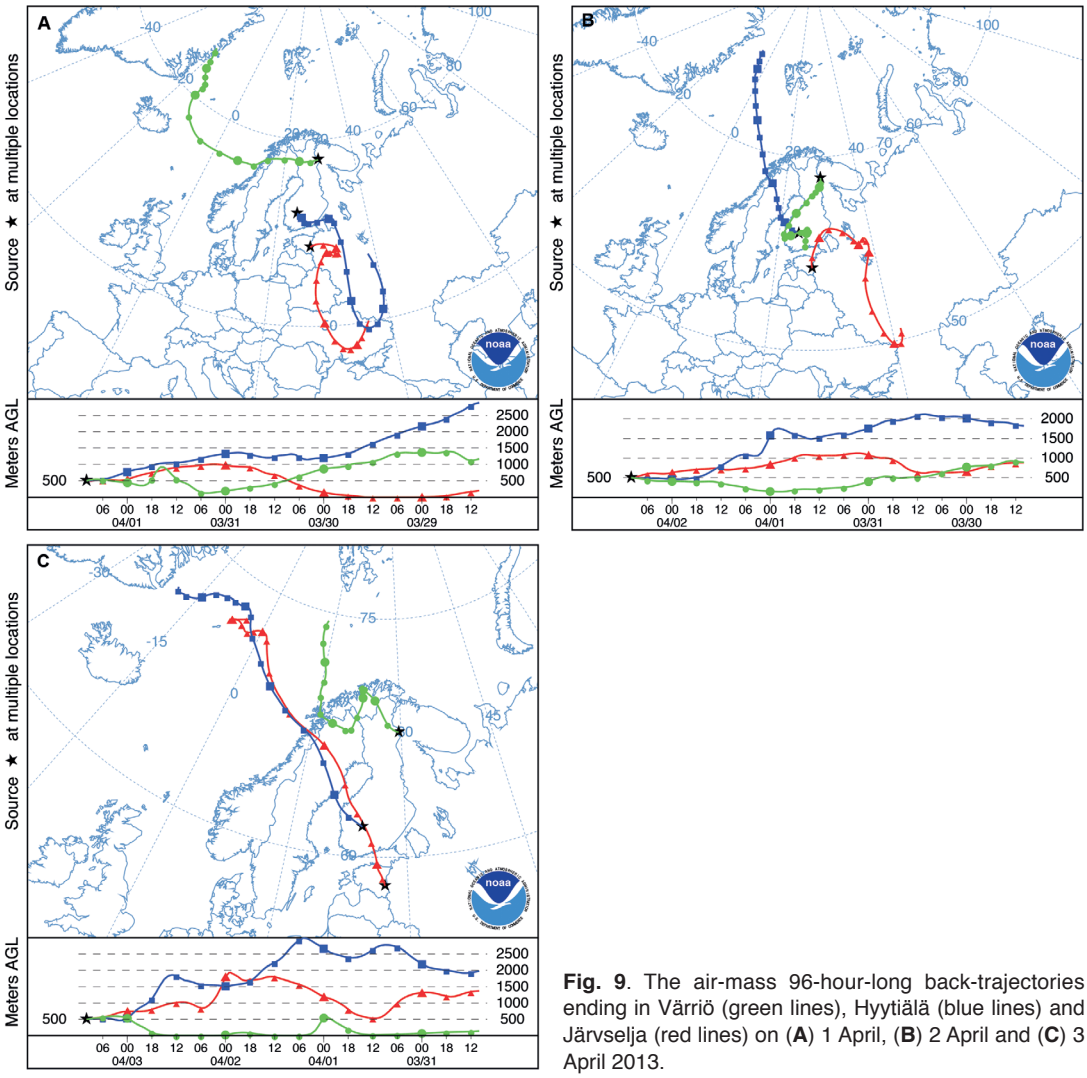


**Fig. 9**. The air-mass 96-hour-long back-trajectories ending in Värriö (green lines), Hyytiälä (blue lines) and Järvselja (red lines) on (**A**) 1 April, (**B**) 2 April and (**C**) 3 April 2013.

nucleation mode particles can be transported also by the air mass during its movement, but the particle growth and the coagulation scavenging diminish their concentration down to zero during next 24 hours. A new nucleation burst is needed to maintain the concentration of nucleation mode particles.

By looking at the Värriö data, it seems that the nucleation mode particles (3–25 nm) had a considerably longer lifetime (elevated concentrations also during nighttime) on 2 April than on the next day (3 April), probably due to their low loss by coagulation. Usually at Järvselja and Hyytiälä, the continuation of the particle growth was not observable on the day following a NPF event day. However, at Värriö, we found a couple of NPF events when particles continued growing during the night to the next day, so that the newly-generated particles affected the size distribution up to 200 nm. During regular NPF events, the size distribution is affected only up to about 100 nm.

## Conclusions

In this study, we compared new-particle-formation (NPF) events occurring at three widely

spaced stations (Värriö, Hyytiälä and Järvselja) during 2013–2014. Our main focus was on discrepancies and similarities among the NPF-event data from different sites, seasonal and inter-annual variations, as well as geographical variation along the north–south transect. The analysis was based on the concentrations and number size distributions of aerosol particles and air ions.

We conclude that the growth rate of nucleation mode particles (3–25 nm) and the apparent source rate of condensable vapors vary along the north to south transect, the highest values being observed at the southernmost station (Järvselja). The condensation sinks and formation rates of 2 and 3 nm particles were almost the same at Hyytiälä and Järvselja, being several times higher as compared with those at Värriö. The frequency of the NPF events was the highest at Hyytiälä, where they were recorded on more than 25% of the days. The frequencies of events at Järvselja and Värriö were about 20% and 9%, respectively. The smaller frequency of events at Järvselja may be due to the different forest structure as compared with that at Hyytiälä, and the lowest frequency at Värriö due to the low source rate of condensable vapors. The mean growth rates (GR) of aerosol particles estimated from the DMPS/EAS measurements for the entire size range of 3–25 nm increased from north to south, having the values of 1.8, 2.5 and 5.4 nm $h^{-1}$ at Värriö, Hyytiäla and Järvselja, respectively. The NAIS spectrometers available in Hyytiälä and Järvselja made it possible to estimate the size dependent growth rates of nucleation mode aerosol particles. The average values of GR were 2.3, 3.8 and 4.6 nm $h^{-1}$ at Hyytiäla and 3.4, 5.2 and 7.1 nm $h^{-1}$ at Järvselja in the size ranges of 1.6–3 nm, 3–7 nm and 7–25 nm, respectively.

The air-mass back-trajectories calculated using HYSPLIT enabled us to find out the variation in NPF parameters along the north to south transect. The most illustrative result was from the analysis of the number concentration of nucleation mode particles (3–25 nm) at the three measurement stations by applying the trajectory statistical method that combines *in situ* measurements of aerosol particle concentrations and back-trajectories. The results showed a variation in the number concentration fields of nucleation mode particles with respect to transport directions of air masses and the dependence of these concentrations along the north to south transect, with the highest concentrations occurring at Järvselja and the lowest ones at Värriö. The study also showed that the highest concentrations occurred at all the stations during the periods when the Arctic air masses moved over measurement locations form northerly directions.

Our results indicate that the NPF events are large-scale phenomena occurring in anticyclonic air masses of horizontal extent up to 1000 km (distance between Järvselja and Värriö) in favorable meteorological conditions. In 2013–2014, there were 26 days with the NPF events occurring simultaneously at all the three stations. Our results indicate that the NPF events at the studied locations were mainly associated with the cold Arctic air inflow (anticyclone) and frontal passage over the stations. Annual variation in the NPF frequency can be explained by changes in the inflow of Arctic air masses and the photochemical activity.

*Acknowledgements*: This work was supported by the Estonian Research Council Projects IUT20-11 and IUT20-52, the European Regional Development Fund through the Environmental Conservation and Environmental Technology R&D Programme project BioAtmos (3.2.0802.11-0043), the "Estonian Research Infrastructures Roadmap" project Estonian Environmental Observatory (3.2.0304.11-0395), the "Internationalization of Science Programme" project INSMEARIN (10.1-6/13/1028), and by the European Research Council (advanced grant 322603, SIP-VOL+). We acknowledge the ACTRIS projects (the European Union's FP7 capacities programme under ACTRIS grant no. 262254, and Horizon 2020 research and innovation programme under ACTRIS-2 grant no. 654109), the Academy of Finland Centre of Excellence (grant no. 272041), and a fellowship from the Nordic Centre of Excellence CRAICC. The authors gratefully acknowledge the NOAA Air Resources Laboratory (ARL) for the provision of the HYSPLIT transport and dispersion model and READY website (http://www.ready.noaa.gov) used in this publication.

## References

Aalto P., Hämeri K., Becker E., Weber R., Salm J., Mäkelä J.M., Hoell C., O'Dowd C.D., Karlsson H., Hansson H.C., Väkevä M., Koponen I.K., Buzorius G. & Kulmala M. 2001. Physical characterization of aerosol particles during nucleation events. *Tellus* 53B: 344–358.

Anderson H.R. 2009. Air pollution and mortality: a history. *Atmos. Environ.* 43: 142–152.

Asmi E., Sipilä M., Manninen H.E., Vanhanen J., Lehtipalo

K., Gagné S., Neitola K., Mirme A., Mirme S., Tamm E., Uin J., Komsaare K., Attoui M. & Kulmala M. 2009. Results of the first air ion spectrometer calibration and intercomparison workshop. *Atmos. Chem. Phys.* 9: 141–154.

Dal Maso M., Kulmala M., Lehtinen K.E.J., Mäkelä J.M., Aalto P. & O'Dowd C.D. 2002. Condensation and coagulation sinks and formation of nucleation mode particles in coastal and boreal forest boundary layers. *J. Geophys. Res.* 107, doi: 10.1029/2001jd001053.

Dal Maso M., Kulmala M., Riipinen I., Wagner R., Hussein T., Aalto P.P. & Lehtinen K.E.J. 2005. Formation and growth of fresh atmospheric aerosols: eight years of aerosol size distribution data from SMEAR II, Hyytiala, Finland. *Boreal Env. Res.* 10: 323–336.

Dal Maso M., Sogacheva L., Aalto P.P., Riipinen I., Komppula M., Tunved P., Korhonen L., Suur-Uski V., Hirsikko A., Kurten T., Kerminen V.-M., Lihavainen H., Viisanen Y., Hansson H.-C. & Kulmala M. 2007. Aerosol size distribution measurements at four Nordic field stations: identification, analysis and trajectory analysis of new particle formation bursts. *Tellus* 59B: 350–361.

Dal Maso M., Sogacheva L., Anisimov M.P., Arshinov M., Baklanov A., Belan B., Khodzher T.V., Obolkin V.A., Staroverova A., Vlasov A., Zagaynov V.A., Lushnikov A., Lyubovtseva Y.S., Riipinen I., Kerminen V.-M. & Kulmala M. 2008. Aerosol particle formation events at two Siberian stations inside the boreal forest. *Boreal Env. Res.* 13: 81–92.

Draxler R.R., & Hess G.D. 1998. An overview of the HYSPLIT_4 modelling system for trajectories, dispersion and deposition. *Austr. Meteorol. Mag.* 47: 295–308.

Fuchs N.A. & Sutugin A.G. 1971. High-dispersed aerosols in topics. *Current Aerosol Research* 2: 1–60.

Gagné S., Lehtipalo K., Manninen H. E., Nieminen T., Schobesberger S., Franchin A., Yli-Juuti T., Boulon J., Sonntag A., Mirme S., Mirme A., Hõrrak U., Petäjä T., Asmi E., Kulmala, M. 2011. Intercomparison of air ion spectrometers: an evaluation of results in varying conditions. *Atmos. Meas. Tech.* 4: 805–822.

Hari P. & Kulmala M. 2005. Station for measuring ecosystem-atmosphere relations (SMEAR II). *Boreal Env. Res.* 10: 315–322.

Heinzerling D. 2004. *Automation of HYSPLIT trajectory generation and subsequent analyses*. Research for Undergraduates Program 2004, Washington University.

Hirsikko A., Laakso L., Hõrrak U., Aalto P.P., Kerminen V.-M. & Kulmala M. 2005. Annual and size dependent variation of growth rates and ion concentrations in boreal forest. *Boreal Env. Res.* 10: 357–369.

Hirsikko A., Bergman T., Laakso L., Dal Maso M., Riipinen I., Hõrrak U. & Kulmala M. 2007. Identification and classification of the formation of intermediate ions measured in boreal forest. *Atmos. Chem. Phys.* 7: 201–210.

Hirsikko A., Vakkari V., Tiitta P., Manninen H.E., Gagne S., Laakso H., Kulmala M., Mirme A., Mirme S., Mabaso D., Beukes J.P. & Laakso L. 2012. Characterisation of sub-micron particle number concentrations and formation events in the western Bushveld Igneous Complex, South Africa. *Atmos. Chem. Phys.* 12: 3951–3967.

Hirsikko A., Nieminen T., Gagne S., Lehtipalo K., Manninen H.E., Ehn M., Hõrrak U., Kerminen V.-M., Laakso L., McMurry P.H., Mirme A., Mirme S., Petäjä T., Tammet H., Vakkari V., Vana M. & Kulmala M. 2011. Atmospheric ions and nucleation: a review of observations. *Atmos. Chem. Phys.* 11: 767–798.

Hõrrak U., Salm J. & Tammet H. 1998. Bursts of intermediate ions in atmospheric air. *J. Geophys. Res.* 103: 13909–13915.

Hõrrak U., Salm J. & Tammet H. 2000. Statistical characterization of air ion mobility spectra at Tahkuse Observatory: Classification of air ions. *J. Geophys. Res.* 105: 9291–9302.

Hõrrak U., Aalto P.P., Salm J., Komsaare K., Tammet H., Mäkelä J.M., Laakso L. & Kulmala M. 2008. Variation and balance of positive air ion concentrations in a boreal forest. *Atmos. Chem. Phys.* 8: 655–675.

Hussein T., Junninen H., Tunved P., Kristensson A., Dal Maso M., Riipinen I., Aalto P.P., Hansson H.-C., Swietlicki E. & Kulmala M. 2009. Time span and spatial scale of regional new particle formation events over Finland and Southern Sweden. *Atmos. Chem. Phys.* 9: 4699–4716.

Iida K., Stolzenburg M.R., McMurry P.H. & Smith J.N. 2008. Estimating nanoparticle growth rates from size-dependent charged fractions: Analysis of new particle formation events in Mexico City. *J. Geophys. Res.* 113: D05207, doi:10.1029/2007JD009260.

Kaasik M., Sofiev M., Prank M., Ruuskanen T., Kukkonen J., Hõrrak U. & Kulmala M. 2011. Geographical origin of aerosol particles observed during the LAPBIAT measurement campaign in spring 2003 in Finnish Lapland. *Boreal Env. Res.* 16: 15–35.

Kazil J., Stier P., Zhang K., Quaas J., Kinne S., O'Donnell D., Rast S., Esch M., Ferrachat S., Lohmann U. & Feichter J. 2010. Aerosol nucleation and its role for clouds and Earth's radiative forcing in the aerosol-climate model ECHAM5-HAM. *Atmos. Chem. Phys.* 10: 10733–10752.

Kerminen V.-M. & Kulmala M. 2002. Analytical formulae connecting the 'real' and the 'apparent' nucleation rate and the nuclei number concentration for atmospheric nucleation events. *J. Aerosol. Sci.* 33: 609–622.

Kristensson A., Johansson M., Swietlicki E., Kivekäs N., Hussein T., Nieminen T., Kulmala M. & Dal Maso M. 2014. NanoMap: Geographical mapping of atmospheric new-particle formation through analysis of particle number size distribution and trajectory data. *Boreal Env. Res.* 19: 329–342.

Kuang C., Chen M., Zhao J., Smith J., McMurry P.H. & Wang J. 2012. Size and time-resolved growth rate measurements of 1 to 5nm freshly formed atmospheric nuclei. *Atmos. Chem. Phys.* 12: 3573–3589.

Kulmala M., Toivonen A., Mäkelä J.M. & Laaksonen A. 1998. Analysis of the growth of nucleation mode particles observed in Boreal forest. *Tellus* 50B: 449–462.

Kulmala M., Petäjä T., Ehn M., Thornton J., Sipilä M., Worsnop D.R. & Kerminen V.-M. 2014. Chemistry of atmospheric nucleation: on the recent advances on precursor characterization and atmospheric cluster composition in connection with atmospheric new particle

formation. *Annu. Rev. Phys. Chem.* 65: 21–37.

Kulmala M., Dal Maso M., Mäkelä J.M., Pirjola L., Väkevä M., Aalto P., Miikkulainen P., Hämeri K. & O'Dowd C.D. 2001. On the formation, growth and composition of nucleation mode particles. *Tellus* 53B: 479–490.

Kulmala M., Petäjä T., Nieminen T., Sipilä M., Manninen H.E., Lehtipalo K., Dal Maso M., Aalto P.P., Junninen H., Paasonen P., Riipinen I., Lehtinen K.E.J., Laaksonen A. & Kerminen V.-M. 2012. Measurement of the nucleation of atmospheric aerosol particles. *Nature Protocols* 7: 1651–1667.

Kulmala M., Riipinen I., Sipilä M., Manninen H.E., Petäjä T., Junninen H., Dal Maso M., Mordas G., Mirme A., Vana M., Hirsikko A., Laakso L., Harrison R.M., Hanson I., Leung C., Lehtinen K.E.J. & Kerminen V.-M. 2007. Toward direct measurement of atmospheric nucleation. *Science* 318: 89–92.

Kulmala M., Kontkanen J., Junninen H., Lehtipalo K., Manninen H.E., Nieminen T., Petäjä T., Sipilä M., Schobesberger S., Rantala P., Franchin A., Jokinen T., Järvinen E., Äijälä M., Kangasluoma J., Hakala J., Aalto P.P., Paasonen P., Mikkilä J., Vanhanen J., Aalto J., Hakola H., Makkonen U., Ruuskanen T., Mauldin R.L.III, Duplissy J., Vehkamäki H., Bäck J., Kortelainen A., Riipinen I., Kurtén T., Johnston M.V., Smith J.N., Ehn M., Mentel T.F., Lehtinen K.E.J., Laaksonen A., Kerminen V.-M. & Worsnop D.R. 2013. Direct observations of atmospheric aerosol nucleation. *Science* 339: 943–946.

Kyrö E.M., Väänänen R., Kerminen V.-M., Virkkula A., Petäjä T., Asmi A., Dal Maso M., Nieminen T., Juhola S., Shcherbinin A., Riipinen I., Lehtipalo K., Keronen P., Aalto P.P., Hari P. & Kulmala M. 2014. Trends in new particle formation in eastern Lapland, Finland: effect of decreasing sulfur emissions from Kola Peninsula. *Atmos. Chem. Phys.* 14: 4383–4396.

Lee Y.H., Pierce J.R. & Adams P.J. 2013. Representation of nucleation mode microphysics in a global aerosol model with sectional microphysics. *Geosci. Model Dev.* 6: 1221–1232.

Leppä J., Anttila T., Kerminen V.-M., Kulmala M. & Lehtinen K.E.J. 2011. Atmospheric new particle formation: real and apparent growth of neutral and charged particles. *Atmos. Chem. Phys.* 11: 4939–4955.

Leppä J., Gagné S., Laakso L., Manninen H.E., Lehtinen K.E.J., Kulmala M. & Kerminen V.-M. 2013. Using measurements of the aerosol charging state in determination of the particle growth rate and the proportion of ion-induced nucleation. *Atmos. Chem. Phys.* 13: 463–486.

Manninen H.E., Petäjä T., Asmi E., Riipinen I., Nieminen T., Mikkilä J., Hõrrak U., Mirme A., Mirme S., Laakso L., Kerminen V.-M. & Kulmala M. 2009. Long-term field measurements of charged and neutral clusters using Neutral cluster and Air Ion Spectrometer (NAIS). *Boreal Env. Res.* 14: 591-605.

Manninen H.E., Nieminen T., Asmi E., Gagné S., Häkkinen S., Lehtipalo K., Aalto P., Vana M., Mirme A., Mirme S., Hõrrak U., Plass-Dülmer C., Stange G., Kiss G., Hoffer A., Törö N., Moerman M., Henzing B., de Leeuw G., Brinkenberg M., Kouvarakis G.N., Bougiatioti A., Mihalopoulos N., O'Dowd C., Ceburnis D., Arneth A., Svenningsson B., Swietlicki E., Tarozzi L., Decesari S., Facchini M.C., Birmili W., Sonntag A., Wiedensohler A., Boulon J., Sellegri K., Laj P., Gysel M., Bukowiecki N., Weingartner E., Wehrle G., Laaksonen A., Hamed A., Joutsensaari J., Petäjä T., Kerminen V.-M. & Kulmala M. 2010. EUCAARI ion spectrometer measurements at 12 European sites — analysis of new particle formation events. *Atmos. Chem. Phys.* 10: 7907–7927.

Mikkonen S., Korhonen H., Romakkaniemi S., Smith J.N., Joutsensaari J., Lehtinen K.E.J., Hamed A., Breider T.J., Birmili W., Spindler G., Plass-Duelmer C., Facchini M.C. & Laaksonen A. 2011. Meteorological and trace gas factors affecting the number concentration of atmospheric Aitken ($D_p$ = 50 nm) particles in the continental boundary layer: parameterization using a multivariate mixed effects model. *Geosci. Model Dev.* 4: 1–13.

Mirme A., Tamm E., Mordas G., Vana M., Uin J., Mirme S., Bernotas T., Laakso L., Hirsikko A. & Kulmala M. 2007. A wide-range multi-channel air ion spectrometer. *Boreal Env. Res.* 12: 247-264.

Mirme S. & Mirme A. 2013. The mathematical principles and design of the NAIS — a spectrometer for the measurement of cluster ion and nanometer aerosol size distributions. *Atmos. Meas. Tech.* 6: 1061–1071.

Mäkelä J.M., Riihelä M., Ukkonen A., Jokinen V. & Keskinen J. 1996. Comparison of mobility equivalent diameter with Kelvin-Thomson diameter using ion mobility data. *J. Chem. Phys.* 105: 1562–1571.

Mäkelä J.M., Aalto P., Jokinen V., Pohja T., Nissinen A., Palmroth S., Markkanen T., Seitsonen K., Lihavainen H. & Kulmala M. 1997. Observations of ultrafine aerosol particle formation and growth in boreal forest. *Geophys. Res. Lett.* 24: 1219–1222.

Nieminen T., Asmi A., Dal Maso M., Aalto P.P., Keronen P., Petäjä T., Kulmala M. & Kerminen V.-M. 2014. Trends in atmospheric new-particle formation: 16 years of observations in a boreal-forest environment. *Boreal Env. Res.* 19 (suppl. B): 191–214.

Nilsson E.D., Paatero J. & Boy M. 2001. Effects of air masses and synoptic weather on aerosol formation in the continental boundary layer. *Tellus* 53B: 462–478.

Noe S.M., Hüve K., Niinemets Ü. & Copolovici L. 2012. Seasonal variation in vertical volatile compounds air concentrations within a remote hemiboreal mixed forest. *Atmos. Chem. Phys.* 12: 3909–3926.

Noe S.M., Kimmel V., Hüve K., Copolovici L., Portillo-Estrada M., Püttsepp Ü., Jõgiste K., Niinemets Ü., Hörtnagl L. & Wohlfahrt G. 2011. Ecosystem-scale biosphere-atmosphere interactions of a hemiboreal mixed forest stand at Jarvselja, Estonia. *For. Ecol. Manage.* 262: 71–81.

Noe S.M., Niinemets Ü., Krasnova A., Krasnov D., Motallebi A., Kängsepp V., Jõgiste K., Hõrrak U., Komsaare K., Mirme S., Vana M. Tammet, H., Bäck J., Vesala T., Kulmala M., Petäjä T. & Kangur A. 2016. SMEAR Estonia: Perspectives of a large-scale forest ecosystem — atmosphere research infrastructure. *Forestry Studies* 63. [In press].

Pope C.A. & Dockery D.W. 2006. Health effects of fine

particulate air pollution: Lines that connect. *J. Air Waste Manage. Assoc.* 56: 709–742.

Rolph G.D. 2016. *Real-time Environmental Applications and Display sYstem (READY)*. NOAA Air Resources Laboratory, College Park, MD. [Available at http://www.ready.noaa.gov].

Riuttanen L., Hulkkonen M., Dal Maso M., Junninen H. & Kulmala M. 2013. Trajectory analysis of atmospheric transport of fine particles, $SO_2$, $NO_x$ and $O_3$ to the SMEAR II station in Finland in 1996–2008. *Atmos. Chem. Phys.* 13: 2153–2164.

Ruuskanen T.M., Kaasik M., Aalto P.P., Hõrrak U., Vana M., Mårtensson E.M., Yoon Y.J., Keronen P., Mordas G., Ceburnis D., Nilsson E.D., O'Dowd C., Noppel M., Alliksaar T., Ivask J., Sofiev M., Prank M. & Kulmala M. 2007. Concentrations and fluxes of aerosol particles during the LAPBIAT measurement campaign in Värriö field station. *Atmos. Chem. Phys.* 7: 3683–3700.

Stein A.F., Draxler R.R, Rolph G.D., Stunder B.J.B., Cohen M.D. & Ngan F. 2015. NOAA's HYSPLIT atmospheric transport and dispersion modeling system. *Bull. Amer. Meteor. Soc.* 96: 2059–2077.

Tamm E., Mirme A., Bernotas T., Kulmala M. & Aalto P. 2003. Calibration of the electrical aerosol spectrometer (EAS). *J. Aerosol Sci.* 34: S1241–S1242.

Tammet H. & Kulmala M. 2005. Simulation tool for atmospheric aerosol nucleation bursts. *J. Aerosol Sci.* 36: 173–196.

Tammet H., Mirme A. & Tamm E. 2002. Electrical aerosol spectrometer of Tartu University. *Atmos. Res.* 62: 315–324.

Tammet H., Hõrrak U. & Kulmala M. 2009. Negatively charged nanoparticles produced by splashing of water. *Atmos. Chem. Phys.* 9: 357–367.

Tammet H., Komsaare K. & Hõrrak U. 2013. Estimating neutral nanoparticle steady-state size distribution and growth according to measurements of intermediate air ions. *Atmos. Chem. Phys.* 13: 9597–9603.

Tammet H., Komsaare K. & Hõrrak U. 2014. Intermediate ions in the atmosphere. *Atmos. Res.* 135: 263–273.

Tunved P., Korhonen H., Ström J., Hansson H.-C., Lehtinen K.E.J. & Kulmala M. 2006a. Is nucleation capable of explaining observed aerosol integral number increase during southerly transport over Scandinavia? *Tellus* 58B: 129–140.

Tunved P., Hansson H.-C., Kerminen V.-M., Ström J., Dal Maso M., Lihavainen H., Viisanen Y., Aalto P.P., Komppula M. & Kulmala M. 2006b. High natural aerosol loading over boreal forests. *Science* 312: 261–263.

Tunved P., Hansson H.-C., Kulmala M., Aalto P., Viisanen Y., Karlsson H., Kristensson A., Swietlicki E., Dal Maso M., Ström J. & Komppula M. 2003. One year boundary layer aerosol size distribution data from five nordic background stations. *Atmos. Chem. Phys.* 3: 2183–2205.

Vakkari V., Laakso H., Kulmala M., Laaksonen A., Mabaso D., Molefe M., Kgabi N. & Laakso L. 2011. New particle formation events in semi-clean South African savannah. *Atmos. Chem. Phys.* 11: 3333–3346.

Vana M., Kulmala M., Dal Maso M., Hõrrak U. & Tamm E. 2004. Comparative study of nucleation mode aerosol particles and intermediate air ions formation events at three sites. *J. Geophys. Res.* 109, doi: 10.1029/2003jd004413.

Vana M., Ehn M., Petäjä T., Vuollekoski H., Aalto P., de Leeuw G., Ceburnis D., O'Dowd C.D. & Kulmala M. 2008. Characteristic features of air ions at Mace Head on the west coast of Ireland. *Atmos. Res.* 90: 278–286.

Vehkamäki H., Dal Maso M., Hussein T., Flanagan R., Hyvärinen A., Lauros J., Merikanto J., Mönkkönen P., Pihlatie M., Salminen K., Sogacheva L., Thum T., Ruuskanen T.M., Keronen P., Aalto P.P., Hari P., Lehtinen K.E.J., Rannik U. & Kulmala M. 2004. Atmospheric particle formation events at Varrio measurement station in Finnish Lapland 1998–2002. *Atmos. Chem. Phys.* 4: 2015–2023.

Väänänen R., Kyrö E.M., Nieminen T., Kivekäs N., Junninen H., Virlikula A., Dal Maso M., Lihavainen H., Viisanen Y., Svenningsson B., Holst T., Arneth A., Aalto P.P., Kulmala M. & Kerminen V.-M. 2013. Analysis of particle size distribution changes between three measurement sites in northern Scandinavia. *Atmos. Chem. Phys.* 13: 11887–11903.

Wehner B., Siebert H., Stratmann F., Tuch T., Wiedensohler A., Petäjä T., Dal Maso M. & Kulmala M. 2007. Horizontal homogeneity and vertical extent of new particle formation events. *Tellus* 59B: 362–371.

Zhang R., Khalizov A., Wang L., Hu M. & Xu W. 2012. Nucleation and growth of nanoparticles in the atmosphere. *Chem. Rev.* 112: 1957–2011.